2018 IEEE/RSJ International Conference on Intelligent Robots and Systems (IROS)
Madrid, Spain, October 1-5, 2018

An Omnidirectional Jumper with Expanded Movability via Steering, Self-Righting and Take-off Angle Adjustment

Sojung Yim, Sang-Min Baek, Gwang-Pil Jung and Kyu-Jin Cho, *Member, IEEE*

***Abstract*— In this paper, we propose an omnidirectional jumper with expanded locomotion capabilities. The mechanisms for four functions—jumping, steering, self-righting and take-off angle adjustment—are designed using only two motors to maximize the jumping performance. Jumping uses the modified active triggering mechanism with one motor. Steering shares this motor and uses the wheel touching the ground. The take-off angle is adjusted by changing the angle between the body and the foot using another motor. Self-righting is possible by utilizing combinations of the movements that occur in the energy storing and angle adjustment processes. With these four functions, the robot is capable of jumping in all directions and can jump anywhere in between the maximum height and maximum distance. It can also jump multiple times by self-righting. The robot, with a mass of 64.4 g, jumps up to 113 cm in vertical height, and 170 cm in horizontal distance. This robot can be deployed to explore various environments. Moreover, the design method to implement more functions than the number of motors can be applied to design other small-scale robots.**

I. Introduction

Jumping is a rapid and efficient locomotion for small-scale animals and robots to pass through rough terrain [1]-[4]. Mimicking the jumping locomotion has been studied for the purpose of enabling robots to overcome obstacles several times larger than their body length [4]-[10]. Kovac et al. [4] designed the miniature 7 g jumping robot that jumps 27 times the body length, Noh et al. [5] designed the flea inspired jumping robot that jumps a height that is 30 times larger than its body length, and Zaitsev et al. [6] designed the locust-inspired miniature jumping robot that jumps 25 times its body length.

In order for jumping robots to be used in practical situations such as planetary exploration, reconnaissance, search and rescue, they should have expanded locomotion capabilities. Robots with expanded locomotion capability can jump in various trajectories, and they can overcome various obstacles in effective ways by selecting a suitable trajectory. Integrating jumping into other locomotion can expand locomotion capabilities by performing multi-modal locomotion such as jump-gliding [11]-[13] and jump-crawling [14]. On the other hand, adding take-off angle adjustment, steering, or self-righting on a jumping robot can also expand locomotion capabilities by complementing jumping locomotion. Take-off angle adjustment can expand the trajectory of the jumping from a single line to a plane, steering can expand trajectory from a plane to a space, and self-righting multiplies the movable space. For these reasons, jumping robots implemented with the aforementioned functions have been developed [15]-[20], as listed in Table I: the MSU jumper [15] can steer and self-right, a bio-inspired jumping robot [16] can steer, adjust its take-off angle, and self-right, and the third generation of JPL robot [17] can steer and adjust its take-off angle. To our knowledge, three additional functions—continuously steering, self-righting, and continuously adjusting take-off angle—have not been fully integrated into a single small-scale jumping robot.

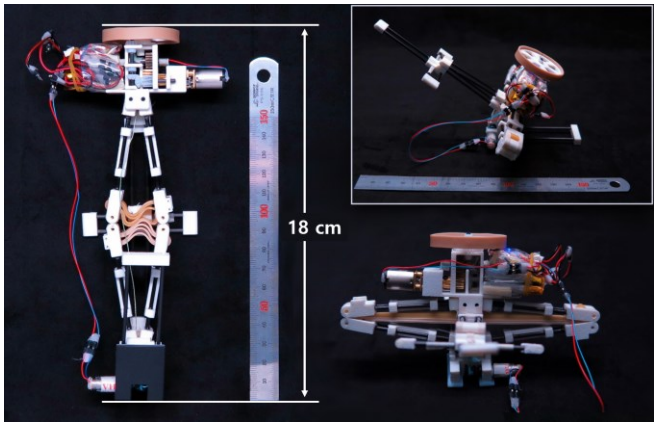

Figure 1. The omnidirectional jumper prototype

This paper presents an omnidirectional jumper capable of steering, self-righting, and take-off angle adjustment (Fig. 1). Implementing additional function in the robot increases the mass, and in small-scale robots, the weight of the actuator accounts for a large portion of the additional mass. As the performance of a jumping robot is inversely proportional to its mass, it is effective to avoid adding actuators to minimize the performance reduction of robots. The omnidirectional jumper is based on the jumping mechanism of JumpRoACH [14] and all four functions — jumping, steering, self-righting, and take-off angle adjustment—are implemented using only two motors. This robot can jump in all directions and maximum jumping height is 113 cm, maximum jumping distance is 170 cm with a mass of 64.4 g.

This paper is structured as follows: The design section describes the mechanism of each function. The result section illustrates the implementation of the functions and demonstration of locomotion in a terrain with obstacles.

* This research was supported by a grant to Bio-Mimetic Robot Research Center Funded by Defense Acquisition Program Administration, and by Agency for Defense Development (UD160027ID).

S. Yim, S. M. Baek and K. J. Cho are with the Biorobotics Laboratory, School of Mechanical Engineering, Seoul National University, Seoul, Republic of Korea.

G. P. Jung is with the Bio-inspired Design Laboratory, School of Mechanical & Automotive Engineering, Seoul National University of Science & Technology, Seoul, Republic of Korea. (corresponding author: 82-2-880-1703, fax: 82-2-880-1663, kjcho@snu.ac.kr)

TABLE I. COMPARISON OF VARIOUS MULTI-FUNCTIONAL JUMPING ROBOTS

Robot	Mass (g)	Size (cm)	Jumping height (cm)	Jumping distance (cm)	Normalized jumping height (cm)	Steering	Take-off angle adjusting	Self-righting	Actuation
MSU jumper [15]	23.5	6.5	87.2	89.8	93.0	YES	NO	YES	1 motor
Bio-inspired jumping robot [16]	154	12	88	30	90.6	YES (360° in 14 steps)	YES (80.33 ~ 86.92°)	YES	2 motors
JPL second generation robot [17]	1300	15	90	200	108	YES	NO	YES	N/A
JPL third generation robot [17]	N/A	N/A	30	N/A	N/A	YES	YES (N/A)	NO	N/A
Steerable miniature jumping robot [18]	14	18	62	21	66	YES	NO	YES	2 motors
Omnidirectional jumper	**64.4**	**18**	**113**	**16**	**115**	**YES**	**YES (40 ~ 87°)**	**YES**	**2 motors**

II. DESIGN

The jumping robot shown in Fig. 2 can perform four functions; jumping, steering, take-off angle adjustment, and self-righting. Integration of additional functions to expand locomotion capabilities increases mass. Therefore, an important issue in designing this robot is to reduce the jumping performance degradation due to additional mass, and our strategy is to minimize the number of actuators. In this study, there are two approaches for designing the robot to use a minimum number of actuators. The first approach is to implement jumping and steering with a single motor, which is done by designing a gearbox in a modified active triggering mechanism. The second approach is to use the coupled motion of the linkage, so a righting linkage is designed to interconnect self-righting mechanism with the jumping linkage to perform self-righting and energy storage simultaneously.

This robot consists of several parts and two motors to implement four functions. There is the jumping linkage, and the modified active triggering mechanism with a head motor is connected above the jumping linkage. A steering wheel is attached to the top of the modified active triggering mechanism. A foot motor and a take-off angle adjusting foot are located at the bottom of the jumping linkage. The righting linkage is connected to the jumping linkage. Detailed descriptions of the modified active triggering mechanism and mechanisms of each function are provided below.

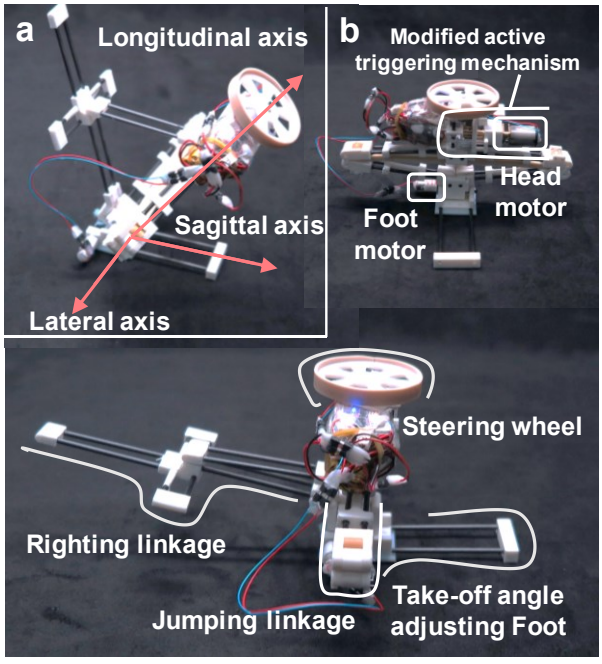

Figure 2. Definition of the (a) axes and (b) part names

A. Modified Active Triggering Mechanism

The modified active triggering mechanism is modified to add steering without additional motors, based on an active triggering mechanism designed to store and actively release energy with a single motor. The active triggering mechanism consists of the head motor, and the gearbox including an actuating gear, a traveling gear, and a winding pulley gear. The traveling gear rotates around the motor in contact with the actuating gear, and engages with or disengages from the winding pulley gear depending on the rotating direction of the motor. When the motor rotates in a clockwise direction as shown in Fig. 3(a), the traveling gear engages with the winding pulley gear, and all three gears rotate together. The motor torque is then transferred to the winding pulley gear, and used for energy storage. When the motor stops, all gears stop rotating and maintain their positions. At this time, when the motor rotates in a counterclockwise direction, the traveling gear disengages from the winding pulley gear, and the motor torque is no longer transmitted to the winding pulley gear. Thus, the winding pulley gear is free to rotate and the stored energy is released.

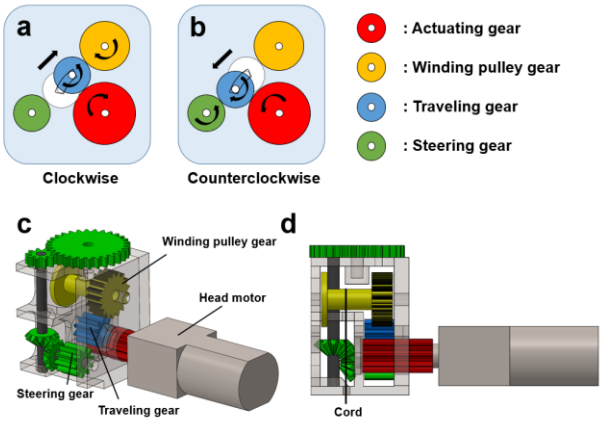

Figure 3. Conceptual diagram of modified active triggering mechanism. (a) Rotating the head motor in clockwise winds the cord and stores energy. (b) Rotating the motor in counterclockwise releases the energy and steers the robot. (c), (d) 3D CAD view of the mechanism

If the motor continues to rotate in the counterclockwise direction, the traveling gear continues to rotate while being separated from the winding pulley gear. The motor torque transmitted at this time is not used, and therefore is used for steering. A steering gear set that is composed of spur gears and bevel gears is added to the active triggering mechanism to utilize the unused motor torque to rotate the steering wheel. Therefore, when the motor rotates counterclockwise and the traveling gear engages with the steering gear, the steering wheel rotates and the robot can steer. Thus, the modified active triggering mechanism enables steering and jumping with the single motor.

B. Jumping Mechanism

The jumping mechanism consists of a rhombus-shaped four-bar linkage, latex bands for energy storage, and the modified active triggering mechanism with the head motor. In a rhombus-shaped four-bar linkage, the latex bands connect one pair of facing joints along the lateral axis and a cord passes the other pair of joints through the longitudinal axis. One end of the cord is fixed to the winding pulley gear as shown in Fig. 3(d), and the other end is fixed to the bottom of the robot. When clockwise rotation of the motor winds the cord to the winding pulley gear, the distance between the two joints passing through the cord decreases, so the jumping linkage become compressed. As a result, the latex band stretches and stores energy. The stored energy is maintained until the motor rotates in the opposite direction; therefore, when the motor rotates counterclockwise, the cord is released, and the linkage is restored to its original shape by the restoring force of the latex bands. Then, the energy stored in the latex band is released, and the robot jumps.

C. Steering Mechanism

Steering can change the jumping direction, so the robot can jump in the desired direction. The steering mechanism consists of the steering wheel and the modified active triggering mechanism. Since the steering wheel is in contact with the ground, the robot heads toward the desired direction while the steering wheel is rotating by the counterclockwise rotation of the head motor.

D. Take-off Angle Adjusting Mechanism

Take-off angle adjustment can change the jumping trajectory. The take-off angle can be adjusted by changing the direction of the reaction force by rotating the body about the lateral axis and varying the body angle defined in Fig. 4(b). The foot motor, a torsional spring, and the take-off angle adjusting foot are included in the take-off angle adjustment mechanism to change the body angle. The motor is fixed to the foot, and one end of the cord wound on the motor pulley is attached to the bottom of the main body. Each end of the torsional spring is fixed to the main body and the foot. Rotating the motor in the counterclockwise direction increases the body angle by winding the cord, and rotating the motor in the clockwise direction unwinds the cord and decreases the body angle by the restoring force of the spring (Fig. 4(b), (c)). To prevent the robot from falling down, the foot is designed with appropriate length so that the projection of the center of mass (CoM) to the ground always be located inside the foot area.

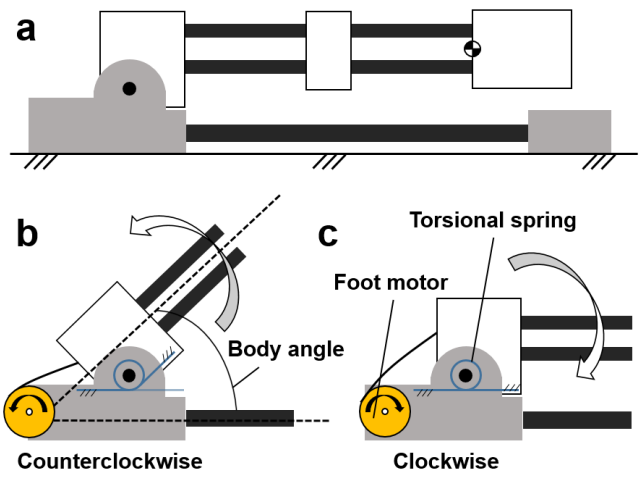

Figure 4. Conceptual diagram of take-off angle adjusting mechanism. (a) Initial posture when the bottom of the foot makes contact with the ground and the body angle is zero. (b) Rotating the foot motor in the counterclockwise increases the body angle. (c) Rotating the motor in the clockwise decreases the angle.

E. Self-righting Mechanism

Self-righting mechanism is required to allow repeated jumps even if the robot lands on the ground in any posture. In the case of this robot, the body shape is designed so that it can always land in two postures. Flat body shape and initially flexed foot allow only front or back side landing. Front side landing denotes the landing posture when the foot is beneath the body, and the back side landing denotes the landing posture when the righting linkage is beneath the body. Self-righting mechanisms of both landing cases are implemented without extra actuators. Descriptions of both landing cases are given below.

1) Front side

As the bottom side of the foot is in contact with the ground on front side landing, front side landing is identical with the case of take-off angle adjustment. Therefore, self-righting of the front side case is performed by operating the foot motor. As there is a limit torque of the motor to raise up the entire body, energy is first stored to reduce the length between the foot joint and the CoM and then upright as shown in Fig. 5(a).

2) Back side

Self-righting of back side landing is implemented by adding only two links. The two links are connected by joints, and the ends of both links are connected to the top and bottom of the jumping linkage so that the motion of the righting linkage interconnect with the motion of the jumping linkage. When the jumping linkage is compressed, the mid joint of the righting linkage protrudes perpendicularly to the plane of the jumping linkage and it pushes against the ground as shown in Fig. 5(b). In order for this linkage not to interfere with other functions, the linkage must be fully folded when the latex bands are in the unstretched state and completely folded when the jumping linkage is entirely compressed. By actuating the head motor, energy storage and righting are performed simultaneously.

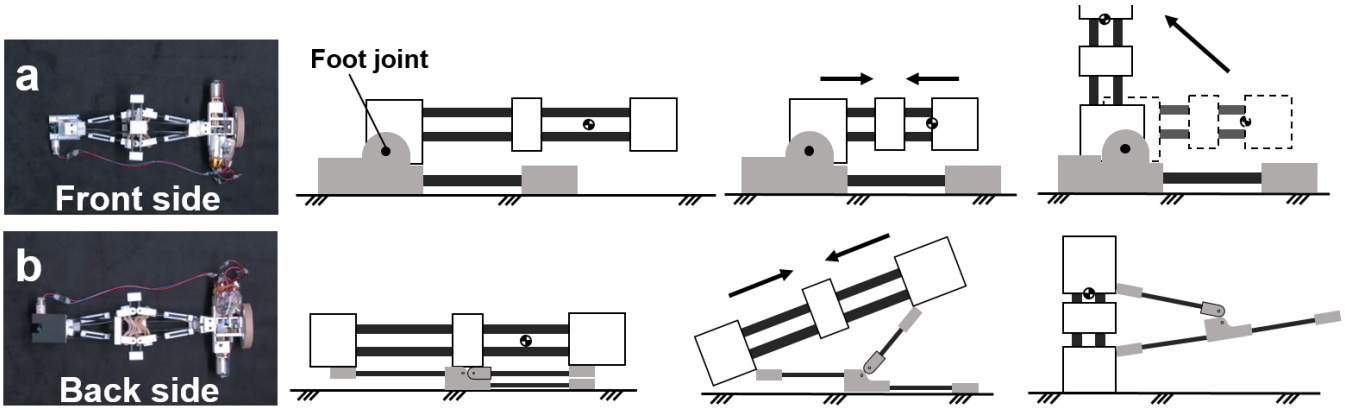

Figure 5. Conceptual diagram of self-righting depending on landing posture. The front and back side landings mean the foot and the righting linkage are located under the body, respectively. (a) Front side landing. First, shorten the length between the CoM and the foot joint, and then upright. (b) Back side landing. The righting linkage pushes against the ground to force the robot into an upright position.

F. *Integration*

As fewer motors are used than the number of functions, the motions used to implement each function are coupled. Therefore, there are predetermined operating sequences for repeated jumps. After the robot lands, the robot first steers. When energy is stored, the motor should be stopped to prevent the winding pulley gear being released, so before storing energy, the steering should be completed by rotating the head motor counterclockwise. Then, the head motor begins to rotate clockwise to store energy. Depending on the landing posture, righting is performed at the same time as energy storing or using the foot motor after completing energy storage. After righting, the desired body angle is set using the foot motor. Then, rotating the head motor in the counterclockwise direction leads to energy release, and the robot jumps. Repeated jumps are possible by repeating the previous steps and a summary of the sequences is as follows.

1) Landing on the front side: steer, energy store, right, adjust take-off angle, and jump

2) Landing on the back side: steer, energy store and right simultaneously, adjust take-off angle, and jump.

The body of the robot is made of 3D printed parts and carbon rods for a light mass. We used a DC motor (Pololu 1000:1 HPCB) as the head motor and another DC motor (D&J LCP06-A03V-0700) as the foot motor. The motors are remotely controlled by small RF controllers (JF24AC). Furthermore, the power is given by two 170 mAh LiPo batteries with 3.7 V.

The mass of the entire robot is 64.4 g, and the mass budget of each function is described in the Table II. The mass of the jumping mechanism is 48.5 g and integration of additional functions increases the mass by 16 g. The size of the body is 180 mm × 90 mm × 30 mm and the height when fully compressed is 70 mm. The length from bottom to CoM is 120 mm when fully released, and 44 mm when fully compressed.

III. Result

Several experiments are performed to test the locomotion capabilities of the jumping robot. The maximum jumping height and distance, trajectories depending on the take-off angle, steering and self-righting performance were examined. Jumping experiments were conducted on a flat ground, and the robot was placed on a rough ground to minimize slippage. The jumping movements were recorded and trajectories were obtained by the open source motion analysis software *Tracker* [21].

TABLE II. Mass Budget of Functions

Function	Mass (g)	Portion (%)
Jumping mechanism	32.9	51.1
Take-off angle adjusting mechanism	8.60	13.4
Steering mechanism	3.30	5.1
Self-righting mechanism	3.96	6.1
Control board, LiPo battery	15.6	24.2
Total	64.4	100

A. *Jumping Performance*

The maximum jumping height and distance were measured to determine the range the jumping robot can reach in a single jump. Jumping performances were calculated as the average of five trials. The maximum jumping height was 113 cm, which is about six times the body length at the take-off angle of 87° and the distance of 16 cm. The maximum jumping distance was 170 cm, which is about nine times the body length at the take-off angle of 60° and the height of 82 cm. The reachable range was between the maximum height and the maximum distance, and Fig. 6(a) illustrates three different trajectories within the reachable range.

B. *Take-off Angle Adjustment*

The direction of the reaction force affects the take-off angle, and as described in the design section, the direction of the reaction force is changed by rotating the body.

As the configurable variable is the body angle, a relationship between the body angle and the take-off angle is required to make the robot jump along a desired trajectory. Therefore, take-off angles for five different body angles (55°, 60°, 70°, 80°, 90°) were obtained (Fig. 6(b)). The take-off angle was calculated as the angle between the ground and the line connecting the point immediately after the robot loses contact with the ground and the point after ten frames (0.04 s).

As shown in Fig. 6(b), the body angle and the take-off angle were positively correlated, so increasing the body angle

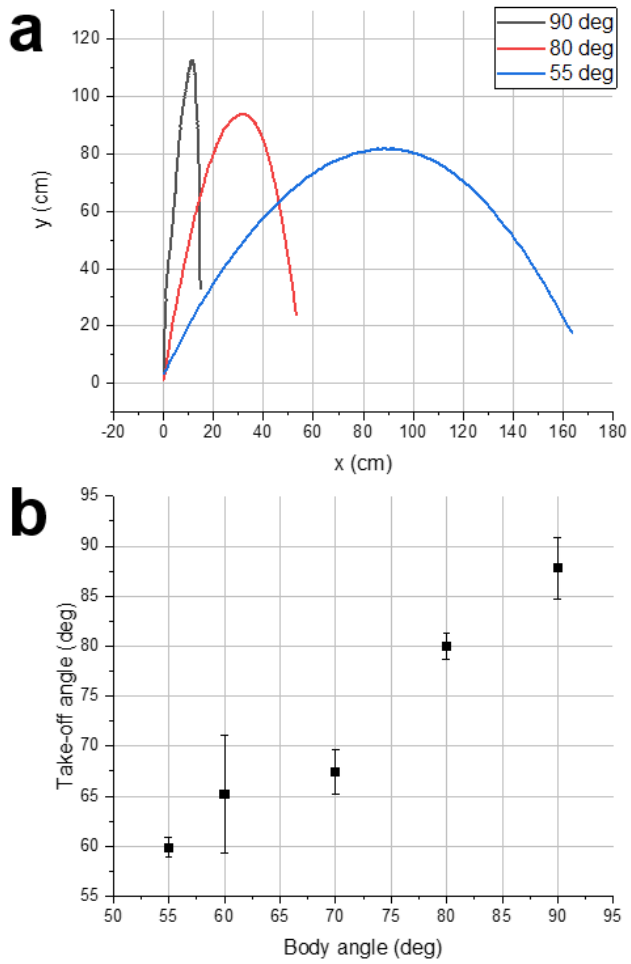

Figure 6. (a) Jumping trajectories in different take-off angle. (b) Comparison of the body angle and the take-off angle.

increased the take-off angle. Errors were small at high body angles and relatively large at small body angles. Furthermore, the take-off angle was larger than the body angle at small body angles.

This might be due to the absence of sufficient friction to prevent slip at low body angles. As the horizontal component of the reaction force is not sufficient for the robot to jump at the body angle, the take-off angle of the robot is larger than the body angle.

When setting the body angle to jump the robot at the desired take-off angle, the body angle can be treated as the take-off angle at high body angles, but calibration between them is required at low angles. This is related to friction, so different calibrations should be applied for different grounds.

C. *Steering*

The steering experiment is performed to test the steering mechanism and verify the robot's performance. Fig. 7 shows the sequence of steering, which can be continuously adjusted over a 360-degree range and it takes 59 s per revolution. As steering uses the counterclockwise rotation of the head motor, the robot can only steer clockwise. The steering speed can be changed by varying the gear ratio of the spur gear at the tip of the bevel gear shaft and the steering wheel gear (Fig. 3(c)).

D. *Self-righting*

The self-righting experiment is conducted to check the self-righting mechanism and its performance. Fig. 8 shows the sequence of self-righting depending on the landing sides. In the case of the front side, energy is stored first and the body is lifted using the foot motor, which takes 53 s. In the case of the back side, the folding righting linkage when storing energy pushes the ground to upright the robot and it takes 58 s. Self-righting can be considered as not time consuming because it works in parallel with energy-storing.

E. *Demonstration on the Terrain with Obstacles*

A demonstration is performed to show that the expanded locomotion capabilities and multiple locomotion allow the robot to traverse various terrains. After falling to the initial position at random, the robot reaches the final position passing through two obstacles of different heights and widths. The two obstacles are 75 cm, 15 cm, and 15 cm, 60 cm in height and width, respectively, and they are 90 cm apart. Fig. 9 shows the trajectory of the jumping robot; it reaches the final position through three jumps. The robot uses its high take-off angle to jump over the first high and narrow barrier, and it uses its low take-off angle to jump over the second low and long barrier. All four functions—jumping, take-off angle adjusting, steering and self-righting—are used for this demonstration.

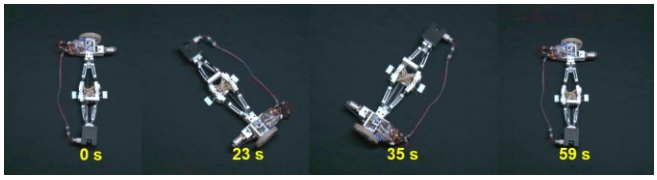

Figure 7. Sequences of steering. It takes 59 s for one revolution

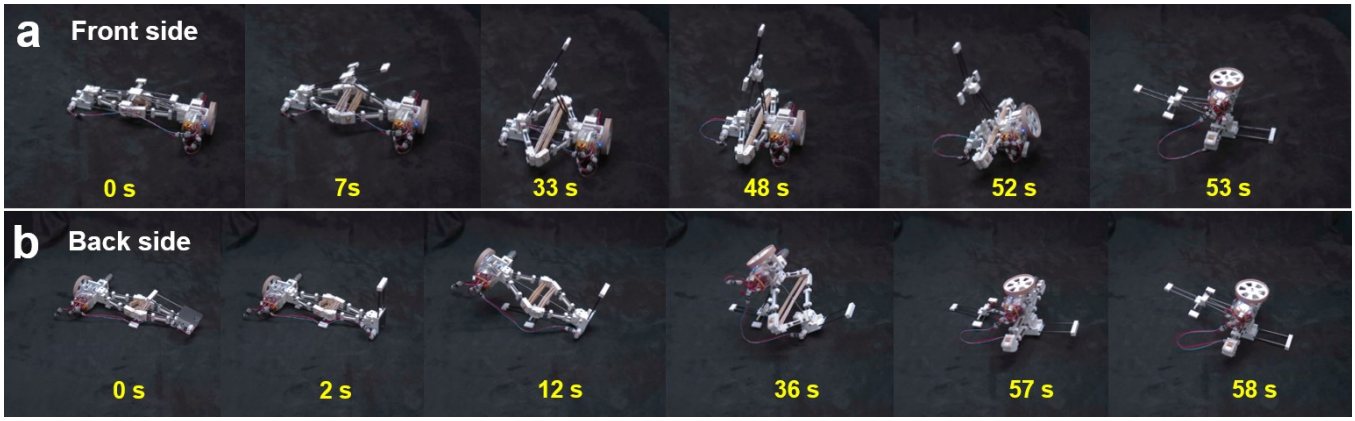

Figure 8. Sequences of self-righting depending on the landing postures. (a) Front side landing takes 53 s to right. (b) Back side landing takes 58 s to right.

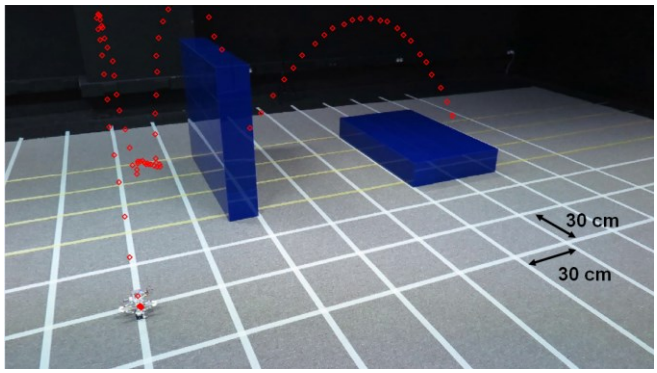

Figure 9. Jumping trajectories on the terrain with obstacles. Three jumps are performed to overcome two obstacles. The obstacles have heights of 75 cm and 15 cm, and distances of 15 cm and 60 cm.

IV. Conclusion

The omnidirectional jumper demonstrates mechanisms of jumping, steering, self-righting, and take-off angle adjustment with only two motors. Jumping is implemented by the modified active triggering mechanism and one motor. The take-off angle is adjusted by the other motor. Steering and self-righting are implemented without additional motors. Steering utilizes the unused range of the active triggering mechanism. Self-righting is possible through motions that occur when other functions are operated. By integrating these functions into one robot, the robot can jump high or low by adjusting the take-off angle depending on the size of obstacles the robot encounters during its mission. Moreover, by steering, the robot can take a detour around a barrier that it cannot jump over.

Experimental results show the reachable range of the jumping robot. The robot has a maximum jumping height of 113 cm with an 87° take-off angle and the distance of 170 cm with a 60° take-off angle, which means it can overcome obstacles having a height six times its body length or having a distance nine times its body length. In addition, the robot steers in 360-degree continuously, so it can head toward any desired direction.

The jumping locomotion on the terrain with obstacles demonstrates that expanded locomotion capabilities by take-off angle adjustment, steering, and multiple jumping by self-righting enable the robot to pass the various obstacles. With these attributes, the jumping robot could be applied to tasks such as planetary exploration and environment monitoring. Moreover, the design principles used to minimize the mass increase could also be used in designing other small-scale robots.

The robot may be improved in future research, as follows: (1) it takes the robot too long time to store energy, steer one revolution and self-right. All three functions are performed using the head motor. The motor has a high gear ratio to provide sufficient force, so it has small rpm. Furthermore, the rhombus-shaped structure is good for large energy-storage capacity; however, the length of the cord to fully compress the jumping linkage is also long. The robot would be more practical if it reduces the time to perform these functions; (2) the original version of the active triggering mechanism has an advantage of changing the amount of energy stored. However, in this version of the robot, the self-righting is coupled with energy storage, and self-righting is completed when energy is fully stored, so the robot cannot change the amount of energy stored. By optimizing the de sign of the self-righting mechanism to allow for adjusting the amount of energy storage, the robot might have more efficient jumping locomotion; and (3) sensing is required in order for this robot to become an autonomous jumping robot. Therefore, sensors to recognize obstacles and a control board to calculate the input data of actuators based on the sensing data should be integrated.

References

[1] R. M. Alexander, *Principles of Animal Locomotion*. Princeton, NJ: Princeton Univ. Press, 2003.

[2] S. Bergbreiter, "Effective and efficient locomotion for millimeter-sized microrobots," in *Proc. IEEE/RSJ Int. Conf. Intell. Robots Syst*., pp. 4030-4035, 2008

[3] R. Armour, K. Paskins, A. Bowyer, J. Vincent, and W. Megill, "Jumping robots: a biomimetic solution to locomotion across rough terrain," *Bioinspi. Biomim.,* vol. 2, no. 3, pp. S65-S82, Jun. 2007.

[4] M. Kovac, M. Fuchs, A. Guignard, J.-C. Zufferey, and D. Floreano, "A miniature 7g jumping robot," in *Proc. IEEE Int. Conf. Robot. Autom.*, pp.583-588, 2008

[5] M. Noh, S.-W. Kim, S. An, J.-S. Koh, and K.-J. Cho, "Flea-inspired catapult mechanism for miniature jumping robots," *IEEE Trans. Robot.,* vol. 28, pp. 1007-1018, Oct. 2012.

[6] V. Zaitsev, O. Gvirsman, U. B. Hanan, A. Weiss, A. Ayali, and G. Kosa, "A locust-inspired miniature jumping robot," *Bioinspir*. *Biomim*., vol. 10, no. 6, p. 066012, Nov. 2015.

[7] D. W. Haldane, M. Plecnik, J. K. Yim, and R. S. Fearing, "Robotic vertical jumping agility via series-elastic power modulation," *Sci. Robot.,* vol. 1, no. 1, Dec. 2016.

[8] F. Li *et al.*, "Jumping like an insect: Design and dynamic optimization of a jumping mini robot based on bio-mimetic inspiration," *Mechatronics,* vol. 22, no. 2, pp. 167-176, Mar. 2012.

[9] M. Wang, X.-z. Zang, J.-z. Fan, and J. Zhao, "Biological jumping mechanism analysis and modeling for frog robot," *J. of Bionic Engineering,* vol. 5, no. 3, pp. 181-188, Sep. 2008.

[10] A. Yamada, M. Watari, H. Mochiyama, and H. Fujimotor, "An asymmetric robotic catapult based on the closed elastica for jumping robot," in *Proc. IEEE Int. Conf. Robot. Autom.,* pp. 232-237, 2008.

[11] A. L. Desbiens, M. T. Pope, D. L. Christensen, E. W. Hawkes, and M. R. Cutkosky, "Design principles for efficient, repeated jumpgliding," *Bioinspi. Biomim*., vol. 9, no. 2, p. 025009, May 2014.

[12] A. Vidyasagar, J. C. Zufferey, D. Floreano, and M. Kovač, "Performance analysis of jump-gliding locomotion for miniature robotics," *Bioinspi. Biomim*., vol. 10, no. 2, p. 025006, Mar. 2015.

[13] M. A. Woodward and M. Sitti, "MultiMo-Bat: A biologically inspired integrated jumping–gliding robot," *Int. J. Robotics Research*, vol. 33, no. 12, pp. 1511-1529, Oct. 2014.

[14] G.-P. Jung, C. S. Casarez, S.-P. Jung, R. S. Fearing, and K.-J. Cho, "An integrated jumping-crawling robot using height-adjustable jumping module," in *Proc. IEEE Int. Conf. Robot. Autom.,* pp. 4680-4685, 2016.

[15] J. Zhao *et al.*, "MSU jumper: A single-motor-actuated miniature steerable jumping robot," *IEEE Trans. Robot.,* vol. 29, pp. 602-614, Jun. 2013.

[16] J. Zhang, G. Song, Y. Li, G. Qiao, A. Song, and A. Wang, "A bio-inspired jumping robot: Modeling, simulation, design, and experimental results," *Mechatronics,* vol. 23, no. 8, pp. 1123-1140, Dec. 2013.

[17] P. Fiorini and J. Burdick, "The development of hopping capabilities for small robots," *Auton. robot.,* vol. 14, no. 2-3, pp. 239-254, Mar. 2003.

[18] M. Kovač, M. Schlegel, J.-C. Zufferey, and D. Floreano, "Steerable miniature jumping robot," *Auton. Robot.,* vol. 28, no. 3, pp. 295-306, Dec. 2010.

[19] J. Zhang, X. Yang, G. Song, Y. Zhang, S. Fei, and A. Song, "Structural-parameter-based jumping-height-and-distance adjustment and obstacle sensing of a bio-inspired jumping robot," *Int. Adv. Robot. Syst.,* vol. 12, no. 6, p. 66, Jan. 2015.

[20] K. Chen, D. Chen, Z. Zhang, and M. Wang, "Jumping robot with initial body posture adjustment and a self-righting mechanism," *Int. Adv. Robot. Syst.,* vol. 13, no. 3, p. 127, Jan. 2016.

[21] D. Brown. (2011) [Online]. *Tracker*. Available: https://physlets.org /tracker/